JOURNAL OF VIROLOGY, Aug. 1997, p. 6183–6190 Vol. 71, No. 8
0022-538X/97/$04.00+0

Generation of Coronavirus Spike Deletion Variants by High-Frequency Recombination at Regions of Predicted RNA Secondary Structure

CYNTHIA L. ROWE,[1] JOHN O. FLEMING,[2] MEERA J. NATHAN,[2] JEAN-YVES SGRO,[3] ANN C. PALMENBERG,[3,4] AND SUSAN C. BAKER[1]*

Department of Microbiology and Immunology and Molecular Biology Program, Loyola University of Chicago, Stritch School of Medicine, Maywood, Illinois 60153[1]; Departments of Neurology and Medical Microbiology, University of Wisconsin and William S. Middleton Veterans Hospital, Madison, Wisconsin 53792[2]; and Institute for Molecular Virology[3] and Department of Animal Health and Biomedical Science,[4] University of Wisconsin, Madison, Wisconsin 53706

Received 10 February 1997/Accepted 29 April 1997

Coronavirus RNA evolves in the central nervous systems (CNS) of mice during persistent infection. This evolution can be monitored by detection of a viral quasispecies of spike deletion variants (SDVs) (C. L. Rowe, S. C. Baker, M. J. Nathan, and J. O. Fleming, J. Virol. 71:2959–2969, 1997). We and others have found that the deletions cluster in the region from 1,200 to 1,800 nucleotides from the 5′ end of the spike gene sequence, termed the "hypervariable" region. To address how SDVs might arise, we generated the predicted folding structures of the positive- and negative-strand senses of the entire 4,139-nt spike RNA sequence. We found that a prominent, isolated stem-loop structure is coincident with the hypervariable region in each structure. To determine if this predicted stem-loop is a "hot spot" for RNA recombination, we assessed whether this region of the spike is more frequently deleted than three other selected regions of the spike sequence in a population of viral sequences isolated from the CNS of acutely and persistently infected mice. Using differential colony hybridization of cloned spike reverse transcription-PCR products, we detected SDVs in which the hot spot was deleted but did not detect SDVs in which other regions of the spike sequence were exclusively deleted. Furthermore, sequence analysis and mapping of the crossover sites of 25 distinct patterns of SDVs showed that the majority of crossover sites clustered to two regions at the base of the isolated stem-loop, which we designated as high-frequency recombination sites 1 and 2. Interestingly, the majority of the left and right crossover sites of the SDVs were directly across from or proximal to one another, suggesting that these SDVs are likely generated by intramolecular recombination. Overall, our results are consistent with there being an important role for the spike RNA secondary structure as a contributing factor in the generation of SDVs during persistent infection.

The genomes of RNA viruses are subject to frequent mutation and RNA recombination events. These genetic alterations enable RNA viruses to rapidly diversify their genomes and adapt to changing environments (20). This diversification can be detected by analysis of the viral quasispecies that evolve after infection and viral replication. Recently, the evolution of RNA viruses has been implicated in the pathogenesis of chronic infections with viruses such as hepatitis C virus (34), measles virus (2), and human immunodeficiency virus (37). Clearly, the lack of an RNA proofreading activity to repair mutations introduced during viral replication can result in the rapid expansion of a viral quasispecies (14). In addition, RNA viruses have been shown to undergo RNA recombination which may radically alter or delete portions of the RNA virus genome (8, 29, 40, 41, 45, 49). Pioneering work with poliovirus recombinants has suggested that recombination of RNA viruses is likely to occur by a copy-choice mechanism involving template switching during replication (25). Three types of copy-choice recombinations can be envisioned for RNA viruses: (i) homologous recombination, in which a nascent strand rebinds at a precisely homologous region on the same or an alternative template; (ii) aberrant homologous recombination, in which the nascent strand rebinds at a downstream site of homology; and (iii) nonhomologous recombination, in which the nascent strand rebinds at a site of nonhomology (26). The generation of recombinant viruses by copy-choice recombination has significant implications for the evolution of a viral quasispecies, escape from vaccine-induced protection, and the potential emergence of unique viral pathogens (15, 36).

The sequences and putative RNA structures which contribute to high-frequency RNA recombination and rapid expansion of viral quasispecies during infection can be studied by using the murine coronavirus mouse hepatitis virus (MHV) (5, 33, 42). MHV is a 32-kb single-stranded RNA virus of positive polarity. The RNA is encapsidated by nucleocapsid proteins and surrounded by a lipid envelope studded with viral glycoproteins. The spike glycoprotein is critical for binding to the MHV receptor (12) and eliciting neutralizing antibodies (13, 17, 48). The spike gene is 4,139 nucleotides (nt) in length and encodes two posttranslational subunits: S1, which is predicted to form the globular head, and S2, which is predicted to form the stalk of the glycoprotein (10, 38). MHV RNA replicates by a unique discontinuous transcription mechanism by which a 3′ coterminal nested set of subgenomic mRNAs is produced (28, 46). This discontinuous RNA synthesis likely contributes to the

* Corresponding author. Mailing address: Department of Microbiology and Immunology, Loyola University of Chicago, Stritch School of Medicine, 2160 S. First Ave., Maywood, IL 60153. Phone: (708) 216-6910. Fax: (708) 216-9574. E-mail: sbaker1@luc.edu.

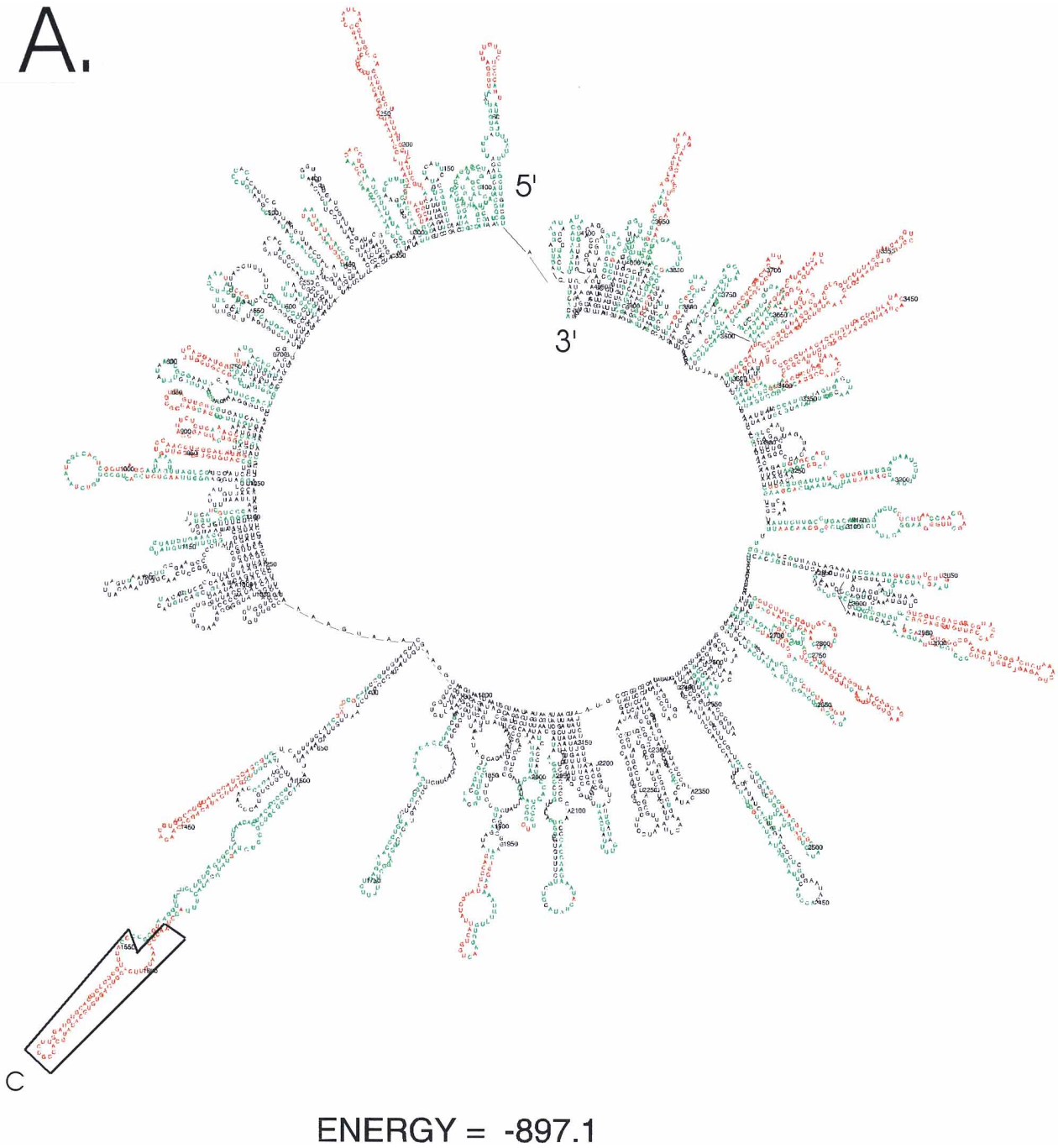

FIG. 1. RNA secondary structure of the 4,139-nt MHV JHM 2.2-V-1 spike glycoprotein predicted by MFOLD. The nucleotide sequence is as described by Taguchi et al. (44), as modified by Wang et al. (47). Folding of the full-length MHV spike RNA sequence for the positive-strand sense (A) and negative-strand sense (B) is shown. The sequence of the probe (boxed area labeled C) used to identify SDVs by differential hybridization (42) is coincident with a predicted isolated stem-loop region.

high-frequency copy-choice RNA recombination observed during MHV infection (5, 33). Indeed, RNA recombination can occur during either positive- or negative-strand RNA synthesis (30). The work of a number of investigators has shown that MHV recombinants arise during passage in tissue culture (22, 24, 27, 32, 33) as well as in inoculated animals (1, 23, 31). Sequence analysis has revealed that the region between 1,200 and 1,800 nt from the 5′ end of the spike RNA, termed the "hypervariable" region, is partially or entirely deleted in a number of MHV isolates (reviewed in reference 42) (Fig. 1). Recently, we found that recombination events which generate viral RNAs with deletions in the spike gene sequence, termed spike deletion variants (SDVs), contribute to the development of a quasispecies in mice inoculated with MHV (42). Interestingly, there was a correlation between the levels of SDVs and disease severity. Mice with the most severe disease harbored

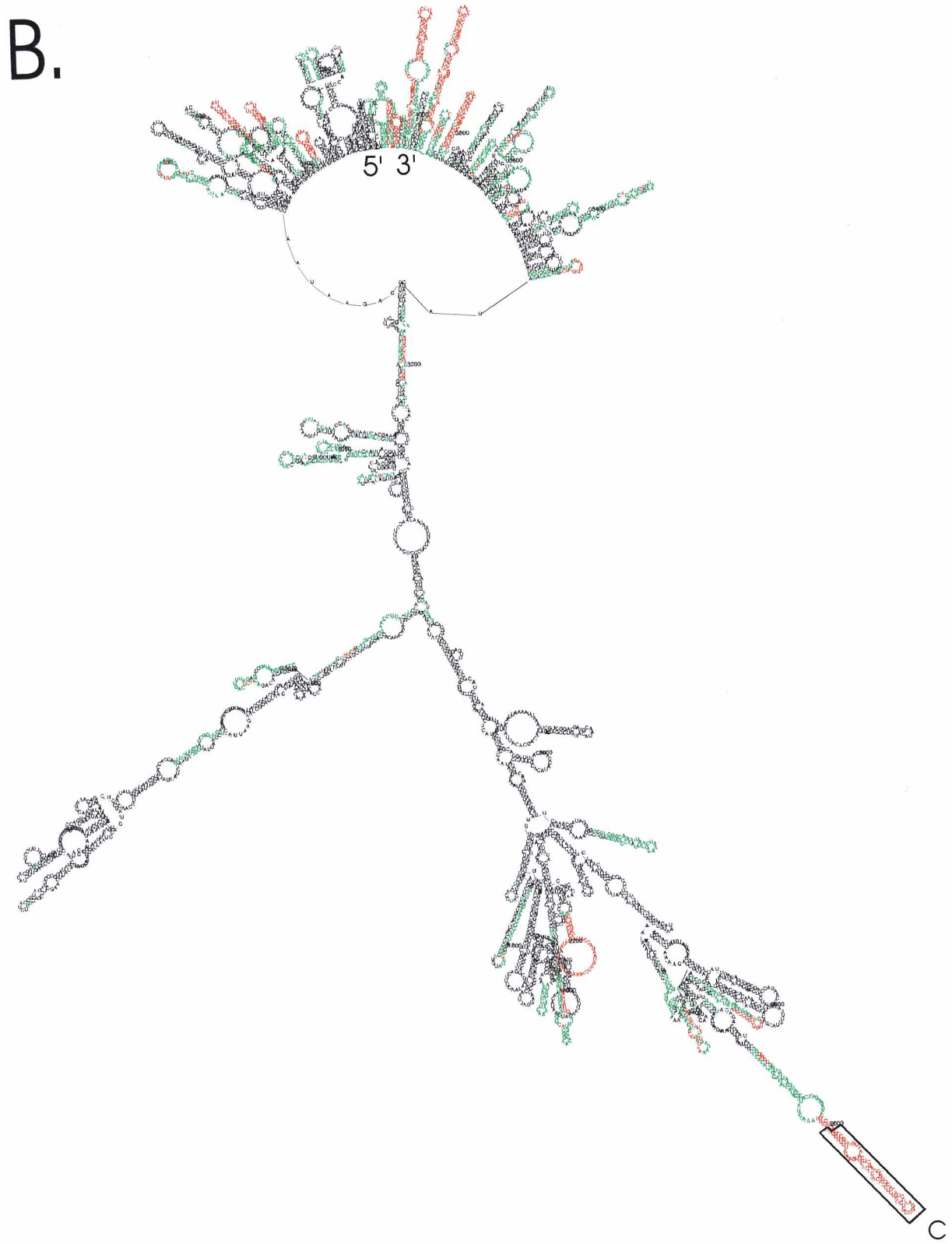

FIG. 1—*Continued.*

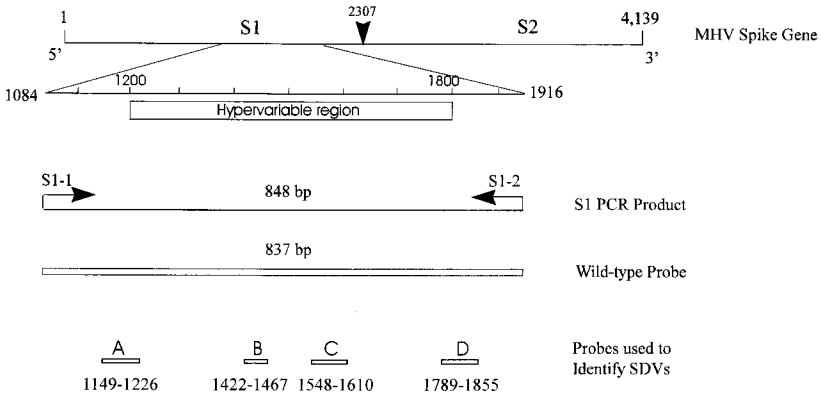

FIG. 2. Illustration of the positions of the PCR primers (S1-1 and S1-2) used to amplify the S1 region and of probes A, B, C, and D and the wild-type probe used to identify SDVs. The wild-type probe was generated as previously described (42). Probes A, B, C, and D were generated by PCR amplification of wild-type S1-containing plasmid DNA with the following primers: probe A (nt 1149 to 1226), S1-7 (5′-GTGCTTTGGTAGTGTCTC-3′) and S1-8 (5′-CCGGAGTTGCCAAT TTGTA-3′); probe B (nt 1422 to 1467), S1-9 (5′-GCGACCTAGCTATTGTC-3′) and S1-10 (5′-AGCGCTAACTATGTCCG-3′); probe C (nt 1548 to 1610), S1-5 (5′-CCATTTGCGCTCGGCAC-3′) and S1-6 (5′-TTGGGTTTACAAGTGCACTC-3′); probe D (nt 1789 to 1855), S1-11 (5′-GATCGCTGCCAAATTTTTGC-3′) and S1-12 (5′-CTGTGGAACACGTAGTC-3′). The following conditions were used to generate the PCR products. One nanogram of the wild-type S1-containing plasmid DNA was mixed with 99 μl of a master mix buffer containing 10 mM Tris-HCl (pH 8.3), 50 mM KCl, 1 mM $MgCl_2$, 800 μM dNTP (800 μM [each] dATP, dCTP, dGTP, and dTTP), an 0.8 μM concentration of each oligonucleotide primer, and 0.5 U of AmpliTaq DNA polymerase (Perkin-Elmer Cetus) in a 100-μl reaction volume. The PCR reaction mixture was subjected to 35 cycles of amplification, with each cycle consisting of 95°C for 30 s, 55°C for 30 s, and 72°C for 30 s. The PCR products were isolated, labeled, and used in differential colony hybridization as previously described (42).

the highest levels and most diverse quasispecies of SDVs. In this study, we wanted to determine whether the SDVs so frequently detected during persistent infection were generated by random recombination events or if the RNA secondary structure was predisposing the spike sequence to specific copy-choice recombination.

To explore the relationship between the spike gene RNA secondary structure and the generation of SDVs, we generated the complete RNA secondary structure fold of the 4,139-nt MHV JHM 2.2-V-1 RNA (accession no., D10235 [44], with point mutations incorporated in accordance with Wang et al. [47]) by using version 2.2 of the MFOLD program (51) (ftp:/ /snark.wustl.edu) (Fig. 1). The MFOLD program determines the global minimum free energy and suboptimal RNA secondary structures by pairing each nucleotide with all possible partners in the sequence following thermodynamic rules and parameters (21). *P*-num (21), the number of all possible pairing partners for each base (within a determined bracket of energy, here 12 kcal), has been extracted and normalized with respect to sequence composition and length (43). Regions with the fewest alternative pairs (low *P*-num values, i.e., less than 3% of the maximum *P*-num for each base at infinite energy) are shown in red. Intermediate *P*-num values are shown in green (between 3 and 6% of the maximum *P*-num), and regions with the highest *P*-num values (above 6% of the maximum *P*-num) are shown in black. For the positive strand, observed *P*-num values range from a minimum value of 2 (base A1569) to a maximum value of 465 (base G1876). After normalization, it was found that 912 (22%) of the 4,139 total bases fell into the red category, 1,302 (31.5%) fell into the green category, and 1,925 (46.5%) fell into the black category. Graphic representations were generated for the global minimum free energy calculated by MFOLD into a PostScript (R) file by the program NAVIEW (7) and were subsequently modified to include color information (43).

Because MHV recombination has been shown to occur during both positive- and negative-strand RNA synthesis (30), we folded the MHV spike RNA sequence in both the positive-strand sense (Fig. 1A) and the negative-strand sense (Fig. 1B). The predicted secondary structure of the spike RNA is striking in that both the positive- and negative-strand RNAs fold to generate a prominent stem-loop structure projecting from a cruciate center. Interestingly, this isolated stem-loop structure coincides with the hypervariable region or recombination "hot spot" (nt 1200 to 1800) which is deleted in a number of MHV variants as described above. Folding the RNA secondary structure of a common deletion variant (in which nt 1524 to 1625 were deleted) revealed that the isolated stem-loop structure was deleted but that the overall secondary structure was essentially unchanged for both positive and negative strands (data not shown). We hypothesized that the isolated stem-loop structure is involved in the high-frequency RNA recombination events that generate MHV SDVs.

To determine if the RNA recombination events which generate SDVs occur throughout the entire S1 region or if the stem-loop structure is a preferred hot spot for recombination, the S1 reverse transcription-PCR (RT-PCR) products generated in our previous study (42) from RNA isolated from the spinal cords of 10 C57BL/6J mice sacrificed after acute (day 4) infection with JHM 2.2-V-1 and 10 mice sacrificed after persistent infection (day 42) were again cloned into pGEM-T and analyzed by differential colony hybridization with probes A, B, C, and D (Fig. 2). Putative SDV clones (i.e., clones that hybridized to the wild-type probe but that did not hybridize to one or more of the internal probes) were analyzed by sequencing as previously described (42).

Table 1 summarizes the data obtained by differential colony hybridization with these probes. Of the 1,614 clones analyzed, 36 SDVs in which the C (core) region alone was deleted were identified. In addition, one SDV in which the B region with the C region was deleted and one double deletion in which a portion of the D region together with the C region was deleted were identified. Interestingly, no SDVs with a deletion in region A, B, or D independent of one in C were detected. This suggests that RNA recombination events which generate SDVs were occurring at a higher frequency in the core region than in regions A, B, and D.

An analysis of these putative SDVs revealed that the percentages of SDVs detected in each mouse were consistent with those from our previous study in which only the C probe was

TABLE 1. Detection of SDVs by differential colony hybridization from the spinal cord RNA of mice infected with MHV JHM[a]

Day PI[b]	Total no. of clones detected with WT probe	No. of nonhybridizing clones detected with probe:			
		A	B	C	D
4	861	0	0	2	0
42	753	0	1[c]	34	1[d]

[a] SDVs were identified from the population of viral RNAs by RT-PCR amplification of the S1 region followed by cloning of the PCR products and differential hybridization of recombinant clones with a wild-type (WT) probe and region-specific probes A, B, C, and D as described in the text. Clones which hybridized to the WT probe but not to one or more of the other four probes were identified as SDVs and characterized by sequencing. No clones in which any region was deleted independently of the C region were identified.

[b] PI, postinfection.

[c] Clone in which the B and C regions were deleted.

[d] Clone in which the C and D regions were deleted.

used to detect SDVs (42). The data are as follows (the numerator indicates the number of SDVs detected and the denominator indicates the total number of clones screened [numbers in parentheses refer to our previous data]): mouse 4-1, 2/67 (2/71); mouse 4-4, 0/61 (1/78); mouse 42-1, 4/88 (5/79); mouse 42-2, 13/63 (17/91); mouse 42-5, 13/81 (9/77); mouse 42-7, 5/60 (3/79); mouse 42-8, 1/80 (3/74). SDVs were not detected in spinal cord samples from mice 4-2, 4-3, 4-5, 4-6, 4-7, 4-8, 4-9, 4-10, 42-3, 42-4, 42-6, 42-9, and 42-10 in either study when >60 clones per RT-PCR sample were screened. Consistent with the hybridization data, sequence analysis revealed essentially the same patterns of SDVs as previously described (42), with two additional patterns identified from mouse 42-7. These SDVs were designated patterns 24 (deletion of nt 1528 to 1616 and 1645 to 1814) and 25 (deletion of nt 1523 to 1650). Overall, these results demonstrate that independent deletion isolates were not detected with probes A, B, and D, indicating that if such SDVs exist, they are much less prevalent in the population than SDVs in which the C region is deleted.

Interestingly, both in-frame and out-of-frame recombination events generating SDVs were detected, indicating that our method is able to identify both potentially productive (in-frame) and nonproductive (out-of-frame) RNA recombination events. Therefore, the functional status of the spike protein was not a limiting factor in the inability to detect SDVs with deletions in regions A, B, or D.

To explore a potential mechanism for the generation of SDVs, we mapped the left and right crossover sites of the 23 previously identified SDV patterns (42) and the two additional SDV patterns identified in this study (patterns 24 and 25) to the predicted RNA secondary structure of the spike gene (Fig. 3). By mapping the SDVs onto the positive- and negative-sense spike RNA secondary structures (Fig. 3A and B, respectively), we found that 13 of the 25 patterns of SDVs cluster at the base of the isolated stem-loop structure. Interestingly, the left and right crossover sites of these SDVs are directly across from or proximal to one another, suggesting that these SDVs were generated by an intramolecular recombination event. Upon encountering this putative secondary structure, the RNA polymerase complex may jump to a spatially proximal template, thereby deleting the hairpin structure. We designated this site high-frequency recombination site 1 or HFR 1 (boxed areas in Fig. 3).

In mapping additional SDVs onto the secondary structure, we noted a second HFR site, HFR 2, at the base of a cruciate structure of the positive-strand RNA (Fig. 3A) or in a region of complex RNA structure in the negative strand (Fig. 3B). The left and right crossover sites for SDV patterns 13, 15, 16, 17, and 21 fall within HFR 2. It has been proposed that complex structures like these are involved in RNA recombination (8, 29, 45). For SDV patterns 12, 14, 18, 19, and 25, one crossover site is located within HFR 1 and the corresponding crossover site is located within HFR 2. This suggests that these regions of extensive RNA secondary structure may be frequent sites of polymerase falling-off and rejoining and likely contribute to the frequent nonhomologous RNA recombination detected in the spike RNA sequence. It is interesting that the HFR sites are adjacent to regions of low *P*-num values (red regions) but that the recombination events seem to occur in regions of intermediate and high *P*-num values (green and black regions, respectively). We speculate that the HFR sites may fold into tertiary structures (that MFOLD is unable to predict) and that such complex structures may facilitate high-frequency RNA recombination. It is currently unclear if coronavirus RNA helicase activity affects high-frequency RNA recombination, as has been shown for brome mosaic virus (35). The hypotheses described above are consistent with the concept of high-frequency RNA recombination occurring in regions of RNA folding (8, 50).

Previous studies have suggested that coronavirus RNA recombination may be random in the absence of selective pressures. Banner et al. demonstrated that intermolecular recombinant spike RNA molecules (with 5′ sequences derived from MHV JHM and 3′ sequences derived from MHV A59) could be detected from coinfected DBT cells. Interestingly, the recombination events clustered to nt 1200 to 1500, the 5′-most portion of the hypervariable region (nt 1200 to 1800) of the spike sequence. The authors initially suggested that an RNA structure may be involved in both recombination and deletion events which generate SDVs (3). However, later studies, in which intracellular populations of recombinant RNAs were compared to passaged viral RNAs, showed that initial RNA recombination occurred randomly over the spike RNA sequence examined. The recombination sites became clustered only after passaging these samples through tissue culture (4), suggesting that recombinants resulted from selection and not RNA recombination hot spots per se. Nevertheless, analysis of MHV recombination frequencies by Fu and Baric revealed that there was a threefold increase in the proportion of recombinations within the S RNA sequence compared to that of the polymerase region (18). Taken together, these studies raised the question of whether SDVs detected during persistent infection were the result of selection of random recombination events or if RNA secondary structure was predisposing the hypervariable region of the spike sequence to specific copy-choice events. In our study, we identified two high-frequency RNA recombination sites and suggest that the majority of the SDVs were derived from intramolecular recombination events during MHV JHM persistence. Intermolecular recombination events may also occur throughout the RNA sequence but likely represent a smaller proportion of the total recombination events detected in persistently infected mice.

It is likely that two factors, (i) coronavirus RNA secondary structure and (ii) host selective pressures, account for the types of SDVs identified in vivo and in vitro. First, RNA secondary structure may contribute to the generation of SDVs by bringing particular regions of the RNA molecule in close proximity and thus providing an opportunity for RNA recombination. Second, host factors may select for the propagation of certain SDVs. For example, in-frame SDVs may bind to tissue-specific receptors, including those recently identified in the central nervous system (11). Also, SDVs which delete the major spike cytotoxic T lymphocyte (CTL) epitope may escape CTL killing

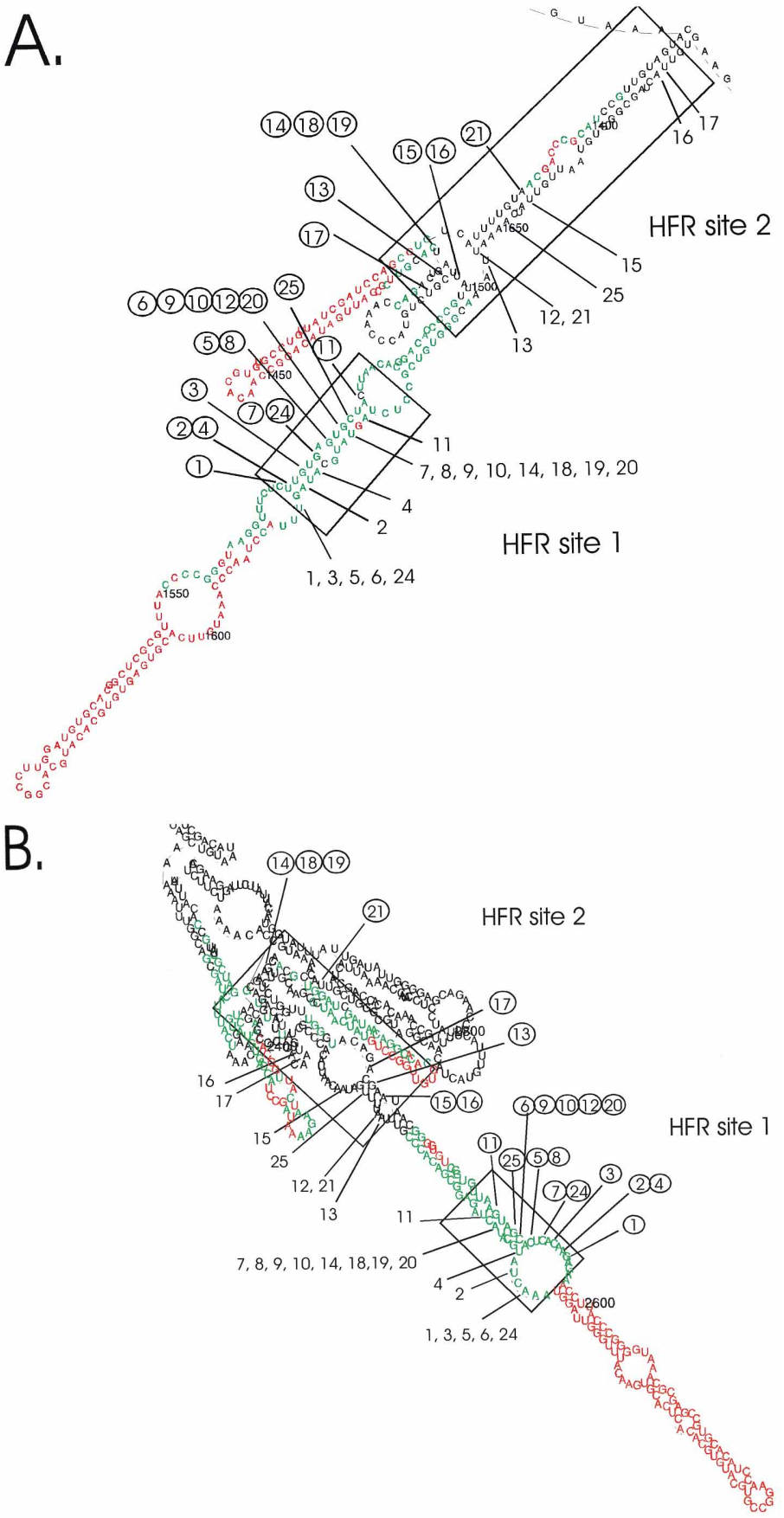
A.
HFR site 2
HFR site 1
14 18 19
21
15 16
13
17
6 9 10 12 20
25
5 8
11
3
7 24
2 4
1
16
17
15
25
12, 21
13
11
7, 8, 9, 10, 14, 18, 19, 20
4
2
1, 3, 5, 6, 24
B.
HFR site 2
HFR site 1
14 18 19
21
17
13
16
17
15 16
6 9 10 12 20
15
25
11
25 5 8
12, 21
3
2 4
7 24
13
11
1
7, 8, 9, 10, 14, 18,19, 20
4
2
1, 3, 5, 6, 24

FIG. 3. Enlargement of the predicted folding of the MHV spike RNA sequence focusing on the isolated stem-loop region. Endpoints of the spike deletion variants which cluster to regions designated HFR site 1 and HFR site 2 are depicted on the positive-strand sense (A) and negative-strand sense (B). The nucleotides bordering the deletion sites of individual SDVs are numbered at the left crossover site (designated by circled numbers) and at the corresponding right crossover site (designated by uncircled numbers). For example, for SDV 1 (in which nucleotides 1533 to 1616 were deleted), left crossover position 1532 and right crossover position 1617 are indicated. (For double deletions, only the core deletion is indicated.)

and thereby continue to replicate during persistent infection (6, 9, 39). In addition, certain SDVs may have reduced cytopathic effects or reduced fusion efficiencies compared to wild-type virus (16, 19). Clearly, one or more of these selective pressures may influence the type of SDVs we detect in persistently infected animals. However, the analysis of out-of-frame SDVs which are not subject to selection pressures provides important information about the relative frequency of spike recombination events. If RNA recombination events occurred with equal frequency throughout the spike sequence, we would have expected to detect deletion variants in all of the regions examined. Remarkably, out-of-frame variants were detected exclusively in the core region (nt 1548 to 1610), suggesting that RNA secondary structure contributes to the S1 hypervariability seen in this region during persistent infection.

Our results illustrate the potential of applying RNA secondary structure analyses to large (>4 kb) RNA sequences to study the complex role of RNA secondary structure in recombination events. Such predictions have been useful in the study of recombination events which generate small defective interfering RNAs (49) and virus-associated RNAs (8). Cascone and coworkers demonstrated that single base mutations that disrupt stem or loop structures eliminated recombination events in turnip crinkle virus (8). Clearly, the most expeditious means of studying the role of the MHV spike RNA secondary structure would be to introduce mutations into a full-length cDNA clone and determine if disruption of the predicted RNA secondary structure alters the frequency or accumulation of deletion variants. However, since no functional cDNA clone is yet available for murine coronavirus, future studies will involve testing the RNA secondary structure prediction provided here within a replication-competent defective interfering RNA.

This work was supported by Public Health Service research grant AI32065 from the National Institutes of Health (to S.C.B.), by National Multiple Sclerosis Society research grant RG2283-A-2, by a Department of Veterans Affairs merit review grant (to J.O.F.), and by a grant from the Lucille P. Markey Charitable Trust (to A.C.P. and J.Y.S.).

We thank Anne Rowley, Tom Gallagher, and Jennifer Schiller for their helpful discussions.

REFERENCES

1. **Adami, C., J. Pooley, J. Glomb, E. Stecker, F. Fazal, J. O. Fleming, and S. C. Baker.** 1995. Evolution of mouse hepatitis virus (MHV) during chronic infection: quasispecies nature of the persisting MHV RNA. Virology **209:** 337–346.
2. **Baczko, K., J. Lampe, U. G. Liebert, U. Brinckmann, V. ter Meulen, I. Pardowitz, H. Budka, S. L. Cosby, S. Isserte, and B. K. Rima.** 1993. Clonal expansion of hypermutated measles virus in a SSPE brain. Virology **197:**188–195.
3. **Banner, L. R., J. G. Keck, and M. M. Lai.** 1990. A clustering of RNA recombination sites adjacent to a hypervariable region of the peplomer gene of murine coronavirus. Virology **175:**548–555.
4. **Banner, L. R., and M. M. Lai.** 1991. Random nature of coronavirus RNA recombination in the absence of selection pressure. Virology **185:**441–445.
5. **Baric, R. S., M. C. Schaad, T. Wei, K. S. Fu, K. Lum, C. Shieh, and S. A. Stohlman.** 1990. Murine coronavirus temperature sensitive mutants. Adv. Exp. Med. Biol. **276:**349–356.
6. **Bergmann, C. C., Q. Yao, M. Lin, and S. A. Stohlman.** 1996. The JHM strain of mouse hepatitis virus induces a spike protein-specific Db-restricted cytotoxic T cell response. J. Gen. Virol. **77:**315–325.
7. **Bruccoleri, R. E., and G. Heinrich.** 1988. An improved algorithm for nucleic acid secondary structure display. Comput. Appl. Biosci. **4:**167–173.
8. **Cascone, P. J., T. F. Haydar, and A. E. Simon.** 1993. Sequences and structures required for recombination between virus-associated RNAs. Science **260:**801–805.
9. **Castro, R. F., and S. Perlman.** 1995. CD8+ T-cell epitopes within the surface glycoprotein of a neurotropic coronavirus and correlation with pathogenicity. J. Virol. **69:**8127–8131.
10. **Cavanagh, D.** 1983. Coronavirus IBV: structural characterization of the spike protein. J. Gen. Virol. **64:**2577–2583.
11. **Chen, D. S., M. Asanaka, K. Yokomori, F. Wang, S. B. Hwang, H. P. Li, and M. M. Lai.** 1995. A pregnancy-specific glycoprotein is expressed in the brain and serves as a receptor for mouse hepatitis virus. Proc. Natl. Acad. Sci. USA **92:**12095–12099.
12. **Collins, A. R., R. L. Knobler, H. Powell, and M. J. Buchmeier.** 1982. Monoclonal antibodies to murine hepatitis virus-4 (strain JHM) define the viral glycoprotein responsible for attachment and cell-cell fusion. Virology **119:** 358–371.
13. **Dalziel, R. G., P. W. Lampert, P. J. Talbot, and M. J. Buchmeier.** 1986. Site-specific alteration of murine hepatitis virus type 4 peplomer glycoprotein E2 results in reduced neurovirulence. J. Virol. **59:**463–471.
14. **Domingo, E., C. Escarmis, N. Sevilla, A. Moya, S. F. Elena, J. Quer, I. S. Novella, and J. J. Holland.** 1996. Basic concepts in RNA virus evolution. FASEB J. **10:**859–864.
15. **Duarte, E. A., I. S. Novella, S. C. Weaver, E. Domingo, S. Wain-Hobson, D. K. Clarke, A. Moya, S. F. Elena, J. C. de la Torre, and J. J. Holland.** 1994. RNA virus quasispecies: significance for viral disease and epidemiology. Infect. Agents Dis. **3:**201–214.
16. **Fazakerley, J. K., S. E. Parker, F. Bloom, and M. J. Buchmeier.** 1992. The V5A13.1 envelope glycoprotein deletion mutant of mouse hepatitis virus type-4 is neuroattenuated by its reduced rate of spread in the central nervous system. Virology **187:**178–188.
17. **Fleming, J. O., M. D. Trousdale, F. A. K. El-Zaatari, S. A. Stohlman, and L. P. Weiner.** 1986. Pathogenicity of antigenic variants of murine coronavirus JHM selected with monoclonal antibodies. J. Virol. **58:**869–875.
18. **Fu, K., and R. S. Baric.** 1992. Evidence for variable rates of recombination in the MHV genome. Virology **189:**88–102.
19. **Gallagher, T. M., S. E. Parker, and M. J. Buchmeier.** 1990. Neutralization-resistant variants of a neurotropic coronavirus are generated by deletions within the amino-terminal half of the spike glycoprotein. J. Virol. **64:**731–741.
20. **Holland, J. J.** 1993. Replication error, quasispecies populations and extreme evolution rates of RNA viruses. Oxford University Press, Oxford, United Kingdom.
21. **Jaeger, J. A., D. H. Turner, and M. Zuker.** 1989. Improved predictions of secondary structures for RNA. Proc. Natl. Acad. Sci. USA **86:**7706–7710.
22. **Keck, J. G., B. G. Hogue, D. A. Brian, and M. M. Lai.** 1988. Temporal regulation of bovine coronavirus RNA synthesis. Virus Res. **9:**343–356.
23. **Keck, J. G., G. K. Matsushima, S. Makino, J. O. Fleming, D. M. Vannier, S. A. Stohlman, and M. M. Lai.** 1988. In vivo RNA-RNA recombination of coronavirus in mouse brain. J. Virol. **62:**1810–1813.
24. **Keck, J. G., S. A. Stohlman, L. H. Soe, S. Makino, and M. M. Lai.** 1987. Multiple recombination sites at the 5′-end of murine coronavirus RNA. Virology **156:**331–341.
25. **Kirkegaard, K., and D. Baltimore.** 1986. The mechanism of RNA recombination in poliovirus. Cell **47:**433–443.
26. **Lai, M. M.** 1992. RNA recombination in animal and plant viruses. Microbiol. Rev. **56:**61–79.
27. **Lai, M. M., R. S. Baric, S. Makino, J. G. Keck, J. Egbert, J. L. Leibowitz, and S. A. Stohlman.** 1985. Recombination between nonsegmented RNA genomes of murine coronaviruses. J. Virol. **56:**449–456.
28. **Lai, M. M., C. L. Liao, Y. J. Lin, and X. Zhang.** 1994. Coronavirus: how a large RNA viral genome is replicated and transcribed. Infect. Agents Dis. **3:**98–105.
29. **Li, Y., and L. A. Ball.** 1993. Nonhomologous RNA recombination during negative-strand synthesis of flock house virus RNA. J. Virol. **67:**3854–3860.
30. **Liao, C. L., and M. M. Lai.** 1992. RNA recombination in a coronavirus: recombination between viral genomic RNA and transfected RNA fragments. J. Virol. **66:**6117–6124.
31. **Luytjes, W., P. J. Bredenbeek, A. F. Noten, M. C. Horzinek, and W. J. Spaan.** 1988. Sequence of mouse hepatitis virus A59 mRNA 2: Indications for RNA recombination between coronaviruses and influenza C virus. Virology **166:** 415–422.
32. **Makino, S., J. O. Fleming, J. G. Keck, S. A. Stohlman, and M. M. Lai.** 1987. RNA recombination of coronaviruses: localization of neutralizing epitopes

and neuropathogenic determinants on the carboxyl terminus of peplomers. Proc. Natl. Acad. Sci. USA **84:**6567–6571.
33. **Makino, S., J. G. Keck, S. A. Stohlman, and M. M. C. Lai.** 1986. High-frequency RNA recombination of murine coronaviruses. J. Virol. **57:**729–737.
34. **Martell, M., J. I. Esteban, J. Quer, J. Genesca, A. Weiner, R. Esteban, J. Guardia, and J. Gomez.** 1992. Hepatitis C virus (HCV) circulates as a population of different but closely related genomes: quasispecies nature of HCV genome distribution. J. Virol. **66:**3225–3229.
35. **Nagy, P. D., A. Dzianott, P. Ahlquist, and J. J. Bujarski.** 1995. Mutations in the helicase-like domain of protein 1a alter the sites of RNA-RNA recombination in brome mosaic virus. J. Virol. **69:**2547–2556.
36. **Novella, I. S., E. Domingo, and J. J. Holland.** 1995. Rapid viral quasispecies evolution—implications for vaccine and drug strategies. Mol. Med. Today **1:**248–253. (Review.)
37. **Nowak, M. A., R. M. May, R. E. Phillips, S. Rowland-Jones, D. G. Lalloo, S. McAdam, P. Klenerman, B. Koppe, K. Sigmund, C. R. Bangham, et al.** 1995. Antigenic oscillations and shifting immunodominance in HIV-1 infections. Nature **375:**606–611.
38. **Parker, S. E., T. M. Gallagher, and M. J. Buchmeier.** 1989. Sequence analysis reveals extensive polymorphism and evidence of deletions within the E2 glycoprotein gene of several strains of murine hepatitis virus. Virology **173:**664–673.
39. **Pewe, L., G. F. Wu, E. M. Barnett, R. F. Castro, and S. Perlman.** 1996. Cytotoxic T cell-resistant variants are selected in a virus-induced demyelinating disease. Immunity **5:**253–262.
40. **Pogany, J., J. Romero, Q. Huang, J. Y. Sgro, H. Shang, and J. J. Bujarski.** 1995. De novo generation of defective interfering-like RNAs in broad bean mottle bromovirus. Virology **212:**574–586.
41. **Romanova, L. I., V. M. Blinov, E. A. Tolskaya, E. G. Viktorova, M. S. Kolesnikova, E. A. Guseva, and V. I. Agol.** 1986. The primary structure of crossover regions of intertypic poliovirus recombinants: a model of recombination between RNA genomes. Virology **155:**202–213.
42. **Rowe, C. L., S. C. Baker, M. J. Nathan, and J. O. Fleming.** 1997. Evolution of mouse hepatitis virus: detection and characterization of S1 deletion variants during persistent infection. J. Virol. **71:**2959–2969.
43. **Sgro, J.-Y., and A. C. Palmenberg.** 1997. Folding of complete viral genomic RNAs. II. Discriminating and visualizing secondary structures. Unpublished data.
44. **Taguchi, F., T. Ikeda, and H. Shida.** 1992. Molecular cloning and expression of a spike protein of neurovirulent murine coronavirus JHMV variant cl-2. J. Gen. Virol. **73:**1065–1072. (Erratum, **73:**2767, 1992.)
45. **Tolskaya, E. A., L. I. Romanova, V. M. Blinov, E. G. Viktorova, A. N. Sinyakov, M. S. Kolesnikova, and V. I. Agol.** 1987. Studies on the recombination between RNA genomes of poliovirus: the primary structure and nonrandom distribution of crossover regions in the genomes of intertypic poliovirus recombinants. Virology **161:**54–61.
46. **van der Most, R. G., and W. J. M. Spaan.** 1995. Coronavirus replication, transcription, and RNA recombination, p. 11–31. *In* S. G. Siddell (ed.), The coronaviridae. Plenum Press, New York, N.Y.
47. **Wang, F. I., J. O. Fleming, and M. M. Lai.** 1992. Sequence analysis of the spike protein gene of murine coronavirus variants: study of genetic sites affecting neuropathogenicity. Virology **186:**742–749.
48. **Wege, H., J. Winter, and R. Meyermann.** 1988. The peplomer protein E2 of coronavirus JHM as a determinant of neurovirulence: definition of critical epitopes by variant analysis. J. Gen. Virol. **69:**87–98.
49. **White, K. A., and T. J. Morris.** 1994. Nonhomologous RNA recombination in tombusviruses: generation and evolution of defective interfering RNAs by stepwise deletions. J. Virol. **68:**14–24.
50. **White, K. A., and T. J. Morris.** 1995. RNA determinants of junction site selection in RNA virus recombinants and defective interfering RNAs. RNA **1:**1029–1040.
51. **Zuker, M.** 1989. On finding all suboptimal foldings of an RNA molecule. Science **244:**48–52.